









RESEARCH ARTICLE

Melanocore uptake by keratinocytes occurs through phagocytosis and involves protease-activated receptor-2 internalization

Hugo Moreiras  | Liliana Bento-Lopes  | Matilde V. Neto |
Cristina Escrevente  | Luís C. Cabaço  | Michael J. Hall  |
José S. Ramalho  | Miguel C. Seabra  | Duarte C. Barral 

CEDOC—Chronic Diseases Research Center, NOVA Medical School (NMS), Faculdade de Ciências Médicas, Universidade NOVA de Lisboa, Lisbon, Portugal

Correspondence

Duarte C. Barral, CEDOC—Chronic Diseases Research Center, NOVA Medical School (NMS), Faculdade de Ciências Médicas, Universidade NOVA de Lisboa, Campo dos Mártires da Pátria 130, 1169-056 Lisbon, Portugal.
Email: duarte.barral@nms.unl.pt

Present address

Hugo Moreiras, The Charles Institute of Dermatology, School of Medicine, University College Dublin, Dublin, Ireland

Funding information

European Commission, Grant/Award Number: 811087; Fundação para a Ciência e a Tecnologia, Grant/Award Numbers: 2020.8812.BD, IF/00501/2014/CP1252/CT0001, PD/BD/114118/2015, PD/BD/137442/2018, PTDC/BIA-CEL/29765/2017, SFRH/BD/131938/2017; FCT / Ministério da Ciência, Tecnologia e Ensino Superior, Grant/Award Numbers: FCT Unit iNOVA4Health - UIDB/04462/2020, UIDP/04462/2020

Abstract

In the skin epidermis, melanin is produced and stored within melanosomes in melanocytes, and then transferred to keratinocytes. Different models have been proposed to explain the melanin transfer mechanism, which differ essentially in how melanin is transferred—either in a membrane-bound melanosome or as a melanosome core, that is, melanocore. Here, we investigated the endocytic route followed by melanosomes and melanosomes during internalization by keratinocytes, by comparing the uptake of melanosomes isolated from the supernatant of melanocyte cultures, with melanosomes isolated from melanocytes. We show that inhibition of actin dynamics impairs the uptake of both melanosomes and melanosomes. Moreover, depletion of critical proteins involved in actin-dependent uptake mechanisms, namely Rac1, CtBP1/BARS, Cdc42 or RhoA, together with inhibition of Rac1-dependent signaling pathways or macropinocytosis suggest that melanosomes are internalized by phagocytosis, whereas melanosomes are internalized by macropinocytosis. Interestingly, we found that Rac1, Cdc42 and RhoA are differently activated by melanocore or melanosome stimulation, supporting the existence of two distinct routes of melanin internalization. Furthermore, we show that melanocore uptake induces protease-activated receptor-2 (PAR-2) internalization by keratinocytes to a higher extent than melanosomes. Because skin pigmentation was shown to be regulated by PAR-2 activation, our results further support the melanocore-based mechanism of melanin transfer and further refine this model, which can now be described as coupled melanocore exo/phagocytosis.

KEYWORDS

macropinocytosis, melanocore, melanosomes, phagocytosis, protease-activated receptor-2

Hugo Moreiras, Liliana Bento-Lopes and Matilde V. Neto contributed equally to this study.

This is an open access article under the terms of the [Creative Commons Attribution-NonCommercial-NoDerivs](https://creativecommons.org/licenses/by-nc-nd/4.0/) License, which permits use and distribution in any medium, provided the original work is properly cited, the use is non-commercial and no modifications or adaptations are made.

© 2022 The Authors. *Traffic* published by John Wiley & Sons Ltd.

1 | INTRODUCTION

Skin pigmentation is the result of the crosstalk between melanocytes and keratinocytes. Melanocytes are highly specialized cells that synthesize the pigment melanin and contact the basal layer of the epidermis. Keratinocytes are present in all the layers of the epidermis and are the final recipients of melanin.¹⁻⁴ Melanin synthesis occurs in specialized organelles called melanosomes, within melanocytes. Melanosomes are lysosome-related organelles, as they share several features with lysosomes, like low pH (at least in early stages), the presence of lysosomal proteins and catalytic enzymes, and are secreted. Once fully mature and located at the tips of melanocyte dendrites, melanosomes are transferred to keratinocytes.⁵⁻⁷ Regarding the mechanism of melanosome transfer from melanocytes to keratinocytes, there are currently four proposed models; cytophagocytosis, membrane fusion, phagocytosis of melanosome-laden globules and coupled exocytosis/endocytosis of the melanin core, or melanocore.⁸⁻¹²

The protease-activated receptor-2 (PAR-2) is one of the few molecular players described to control melanin transfer both *in vivo* and *in vitro*. Moreover, it is known that PAR-2 stimulation leads to the enhancement of melanin transfer, as well as keratinocyte phagocytosis.¹³⁻¹⁷ In addition, we showed that PAR-2 regulates the uptake of melanosomes, but not melanocores.¹⁸ Nonetheless, it is not clear what is the route followed by melanin to enter keratinocytes. The models of shed melanosome-laden globules and coupled exocytosis/endocytosis of melanosomes are the ones that received more attention during recent years and for which there is stronger published evidence.^{18,19} In these models, the pigment is transferred either as a globule containing multiple melanosomes or as “naked” melanin, respectively. Melanosome size varies from 0.5 to 0.8 μm in diameter and could reach a maximum of 2 μm in certain pathological conditions such as ocular albinism and Chediak-Higashi syndrome.²⁰ Therefore, phagocytosis and macropinocytosis are the internalization routes that allow the uptake of such large cargo.^{21,22} Moreover, while macropinocytosis is a general process performed by most cells to take up nutrients from the surrounding environment, phagocytosis is performed mainly by professional phagocytic cells and is usually specific for engulfed cargo, as it is receptor-mediated. Both these routes are highly dependent on actin cytoskeleton remodeling for phagosome and macropinosome cup formation.²³ Regarding the molecular players involved in these two processes, they are mostly shared. Indeed, both pathways are largely dependent on members of the Rho family of small GTPases, namely Rac1, Cdc42 and RhoA that induce actin polymerization and membrane ruffling. Membrane remodeling is spatiotemporally coordinated by the activation of Rho GTPases through the interaction with actin nucleating proteins. Rho effector proteins such as p21-activated kinase (PAK), in the case of Rac1 and Cdc42, and Rho-associated protein kinase, in the case of RhoA, are pivotal for the actin remodeling functions of Rho GTPases.²⁴ In phagocytosis, Cdc42-Rac1 sequential activation is essential for pseudopod formation during membrane extension.²⁵⁻²⁷ However, later steps, including membrane closure, rely on Rac1 activity but require progressive Cdc42 inactivation.²⁶ On the other hand, the role of RhoA in

phagocytosis initiation was suggested to be receptor-dependent. Several reports have shown that Fc-receptor-mediated phagocytosis does not require RhoA activity, whereas its activation is indispensable for complement receptor-mediated phagocytosis.²⁸ Furthermore, it remains controversial whether RhoA contributes to phagosome maturation.²⁸⁻³⁰ In the case of macropinocytosis, Rac1 activity is required not only for the formation of actin-rich membrane ruffles but also in later steps, for membrane scission.^{31,32} Nevertheless, Rac1 must be inactivated to allow macropinosome closure.^{32,33} The requirement of Cdc42 for macropinocytosis has not been clearly established. Despite being found in macropinocytic cups in some cell types, Cdc42 activity was found to be dispensable for the formation of these structures, suggesting it may play only a supportive role in macropinocytosis.^{32,34,35} In addition, a burst of RhoA activity is required during membrane closure in macropinocytosis.³⁶ Macropinosome fission from the plasma membrane is specifically dependent on PAK1-dependent recruitment of Brefeldin A-ADP ribosylated substrate (CtBP1/BARS), after cargo engulfment.^{37,38} Finally, the inhibition of Na⁺/H⁺ exchange by amiloride has been shown to block macropinocytosis.³⁹

Our goal in this study was to further dissect the mechanisms behind melanin internalization by keratinocytes. In particular, we wanted to find out whether these mechanisms differ according to the type of melanin presented to keratinocytes. To address this, we took advantage of an *in vitro* melanin uptake assay previously established by us,¹⁸ in which we isolate melanosomes with intact membranes from MNT-1 melanocytes and melanocores from MNT-1 conditioned medium. We show that the internalization of melanocores, that is, the melanin core devoid of surrounding membrane, is Rac1- and Cdc42-dependent, and CtBP1/BARS- and RhoA-independent, whereas the uptake of melanosomes, that is, melanin core with intact surrounding membrane, is CtBP1/BARS- and RhoA-dependent, and Rac1- and Cdc42-independent. Moreover, we observed that only melanosome internalization is significantly impaired upon treatment with an amiloride derivative, namely 5-(*N*-ethyl-*N*-isopropyl)-amiloride (EIPA), which inhibits macropinocytosis. In addition, Cdc42 shows increased activation in response to melanocore stimulation, whereas RhoA activity increase is higher upon exposure to melanosomes. Furthermore, we show that melanocore uptake induces PAR-2 internalization by keratinocytes to a higher extent than melanosomes. Thus, our results further support the model of coupled exocytosis/endocytosis and indicate that melanocore internalization occurs through phagocytosis in a PAR-2-dependent manner.

2 | RESULTS

2.1 | Melanocore uptake is dependent on actin polymerization

To determine the mechanism by which melanin is internalized, we started by probing for the dependency on actin by using the actin polymerization inhibitory drugs cytochalasin D and latrunculin A. To

ingest particles by phagocytosis and extracellular fluid by macropinocytosis, cells form plasma membrane protrusions that close at their distal end, giving rise to membrane-bound organelles termed phagosomes or macropinosomes, respectively.^{27,37} Because of the size of the protrusions formed during these internalization processes, actin cytoskeleton remodeling is essential to reshape and extend the plasma membrane. Since melanosome size is around 0.5 μm , it is likely that melanin is internalized through phagocytosis or macropinocytosis.²⁰ Therefore, actin polymerization inhibition is expected to impair melanin internalization. To test this hypothesis, we treated XB2 mouse keratinocytes with latrunculin A or cytochalasin D for 1 h and then incubated the cells with melanosomes isolated from the culture medium of MNT-1 melanoma cells (Figure S1) for 24 h in the presence of the drugs. Finally, cells were washed and left to recover their morphology for 1 h to allow melanin quantification by microscopy. We found that both cytochalasin D and latrunculin A lead to a $\sim 30\%$ reduction in the number of melanosomes internalized by keratinocytes, when compared with non-treated cells or cells treated with dimethyl sulfoxide (DMSO; Figure 1). In addition, we found that the internalization of melanosomes isolated from MNT-1 melanocytes (Figure S1) is also dependent on actin polymerization (Figure 2) because the treatment with cytochalasin D or latrunculin A results in a 30% reduction in internalized melanosomes, relative to control cells. However, it is important to note that the observed 30% reduction in melanin uptake is not higher, likely due to the need of a washout step for the cells to recover their morphology and allow proper melanin quantification by microscopy. Nonetheless, the effect observed demonstrates the crucial role that actin plays in melanin uptake by keratinocytes. Therefore, these results show that melanin uptake is at least partially actin-dependent, regardless of the form of melanin presented to the cells.

2.2 | Melanosome internalization is impaired by Rac1 interference or Cdc42 silencing, but not macropinocytosis blockade

Phagocytosis and macropinocytosis play key roles during development and although they are essential mechanisms of internalization dependent on the actin cytoskeleton, there are important differences between them. Phagocytosis allows the internalization of large extracellular particles, while macropinocytosis is used by cells to take up extracellular fluid and soluble cargo from the surrounding environment.^{21,22} Regarding the molecular players involved in these two processes, they overlap significantly, because both are largely dependent on the remodeling of cortical actin for cargo engulfment. The major difference is that macropinocytosis is a general process performed by most cells to take up nutrients from the extracellular milieu, while phagocytosis is mainly performed by specialized cells and is usually specific for the particles engulfed as it is receptor-mediated. Nevertheless, keratinocytes were shown to possess phagocytic ability.^{16,40,41} To characterize the endocytic route followed by melanin, we silenced Rac1, Cdc42, RhoA or CtBP1/BARS in XB2 keratinocytes

(Figure S2), before incubating them for 24 h with melanosomes or melanosomes. We also treated the cells with a Rac1 inhibitor, 5-(5-(7-(Trifluoromethyl)quinolin-4-ylthio)pentyl)oxy)-2-(morpholinomethyl)-4H-pyran-4-one dihydrochloride (EHT 1864), or with a macropinocytosis inhibitor, EIPA, before incubation with melanosomes or melanosomes. The results showed a significant decrease in the uptake of melanosomes upon Rac1 silencing or treatment with EHT 1864 (82% and 70%, respectively), comparing with control cells (Figure 3A–D). Interestingly, treatment with EHT 1864 was confirmed to impair significantly membrane ruffling, as shown by fluorescence microscopy analysis of phalloidin stained cells (Figure S2). Moreover, CtBP1/BARS depletion or macropinocytosis inhibition do not affect melanosome internalization (Figure 3A–D). As expected, we observed that melanosome, but not melanosome internalization is dependent on PAR-2, confirming our previous studies (Figures 3A,B and 4A,B).¹⁸ On the other hand, upon CtBP1/BARS depletion or treatment with EIPA, we observed a significant decrease in the internalization of melanosomes (35% and 55%, respectively), comparing with control cells, whereas Rac1 depletion/inhibition does not affect melanosome uptake (Figure 4A–D). Interestingly, we observed that Cdc42 is required for melanosome, but not melanosome internalization (56% vs. 5% decrease, respectively, upon silencing of Cdc42) (Figures 3E,F and 4E,F), whereas RhoA silencing impacts mostly melanosome internalization (52% decrease vs. 26%, in the case of melanosomes) (Figures 3G,H and 4G,H).

To confirm these results, we used as a positive control 70 kDa dextran, which was shown to be internalized predominantly via macropinocytosis in an amiloride-sensitive manner.⁴² In this case, we quantified melanin internalization by immunofluorescence, staining melanin-containing compartments (named by us melanokerasomes)¹¹ in keratinocytes with an antibody against premelanosome protein (PMEL), an essential structural protein in melanosome biogenesis. Importantly, both melanosomes and melanosomes within keratinocytes are stained using this antibody (Figure S3A), allowing the accurate quantification of melanokerasomes. Strikingly, EIPA treatment reduces melanosome internalization by 55%, similar to the decrease observed for dextran ($\sim 56\%$) (Figure S3B). As expected, CtBP1/BARS depletion significantly impairs dextran internalization ($\sim 32\%$), confirming that it occurs via macropinocytosis (Figure S3C). In contrast, we found that melanosome uptake is almost unaffected by EIPA treatment (Figure S3C), further suggesting that melanosomes are not internalized by macropinocytosis. Altogether, these results indicate that melanosome internalization occurs through phagocytosis, whereas melanosomes are internalized through macropinocytosis.

2.3 | Cdc42 and RhoA are differently activated by melanosomes and melanosomes

To better understand the sequence of events involved in melanosome and melanosome internalization, we evaluated the activation of Rho GTPases. These proteins are quickly and transiently activated in response to different stimuli. Maximal activation ranges from few seconds to several minutes, with a decline in the activity thereafter.

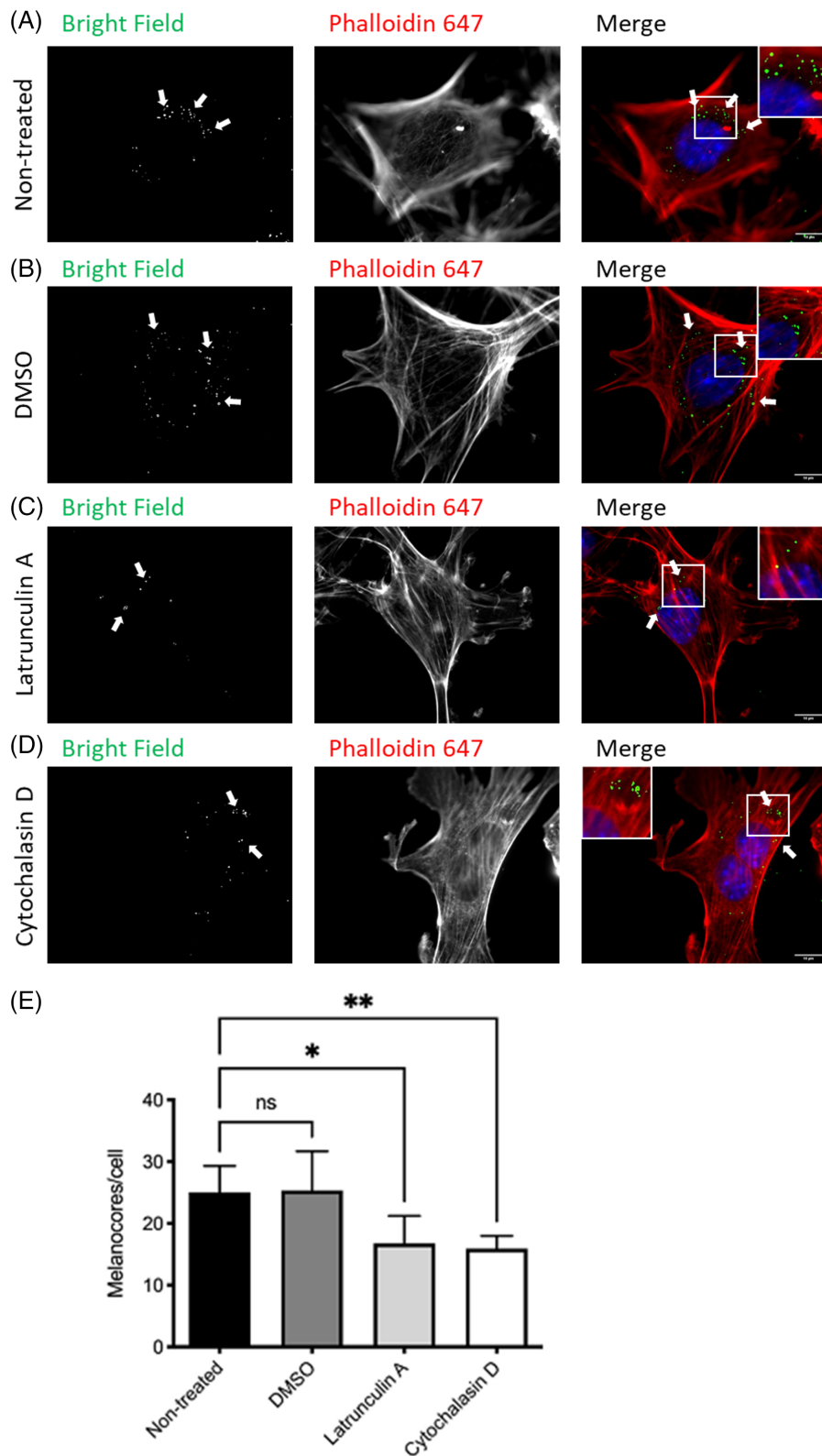
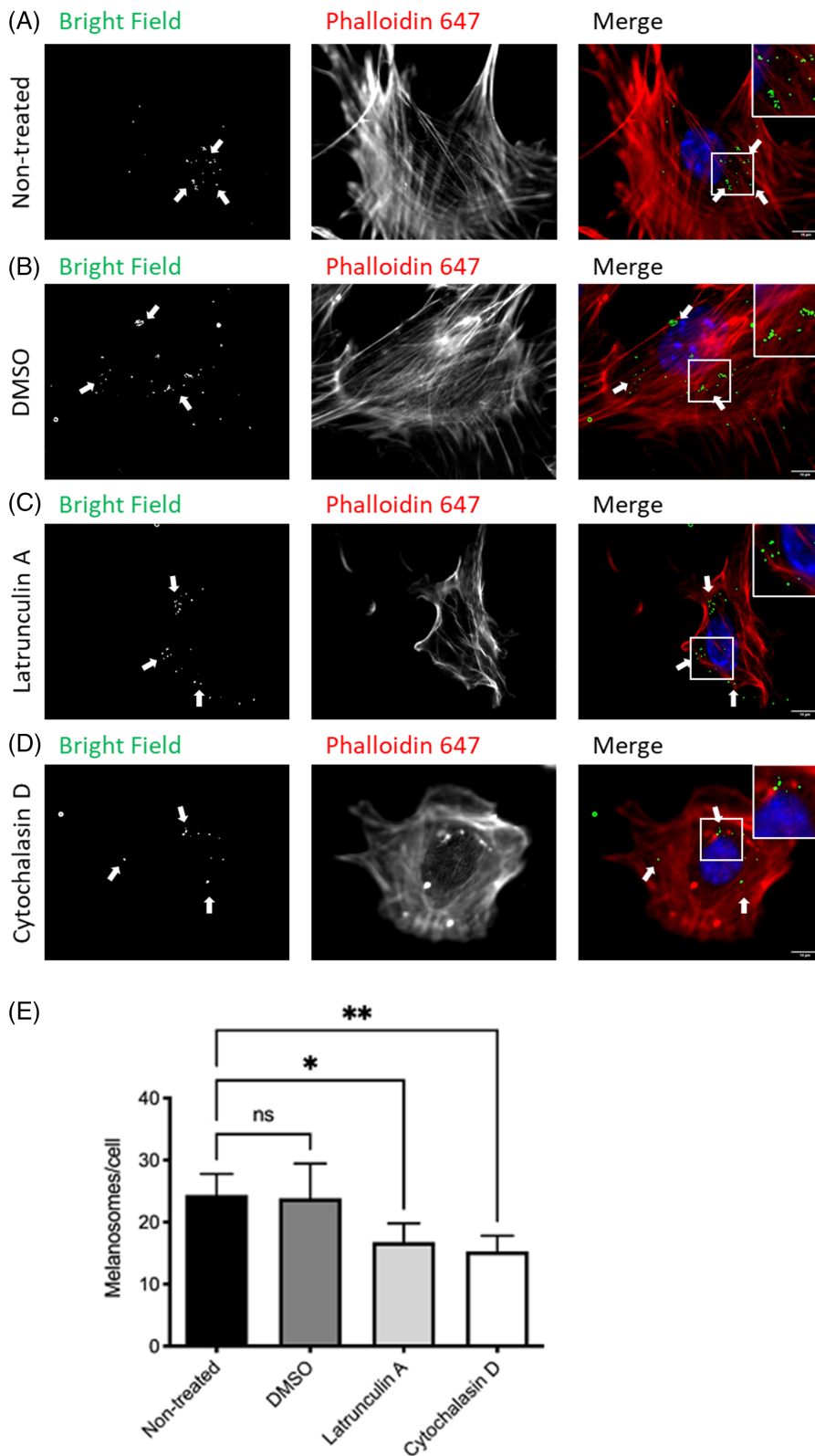


FIGURE 1 Melanocore uptake by keratinocytes is actin-dependent. XB2 mouse keratinocytes were (A) left untreated or treated with (B) dimethyl sulfoxide (DMSO, vehicle), (C) Latrunculin A, or (D) Cytochalasin D for 1 h and then incubated with melanocores for 24 h. Cells were washed and allowed to recover for 1 h before fixation to allow melanin quantification by microscopy. Nuclei were visualized by 4',6-diamidino-2-phenylindole (DAPI) staining (blue), F-actin stained with Phalloidin 647 (red) and melanocores pseudocolored in green from bright field images. Arrows show melanocores internalized by keratinocytes. Scale bars = 10 μ m. (E) Quantification of melanocore number per cell. *p* values (one-way ANOVA) were considered statistically significant when <0.05 (*), <0.01 (**), or non-significant (ns) when ≥ 0.05 . Plots show mean \pm SD of three independent experiments

Activation of Rac1, Cdc42 or RhoA results in characteristic changes in the actin cytoskeleton.^{25,43} For instance, Rac1 activation induces the formation of actin-rich lamellipodia and membrane ruffles.⁴³ When Cdc42 is active, prominent membrane extensions termed filopodia

and smaller microspikes are formed, whereas RhoA activation results in increased formation of stress fibers.⁴³ Hence, we first optimized the timepoint in which we could observe the formation of actin-rich structures in response to the presence of either melanocores or

FIGURE 2 Melanosome uptake by keratinocytes is actin-dependent. XB2 mouse keratinocytes were (A) left untreated or treated with (B) dimethyl sulfoxide (DMSO, vehicle), (C) Latrunculin A, or (D) Cytochalasin D for 1 h and then incubated with melanosomes for 24 h. Cells were washed and allowed to recover for 1 h before fixation to allow melanin quantification by microscopy. Nuclei were visualized by 4',6-diamidino-2-phenylindole (DAPI) staining (blue), F-actin stained with Phalloidin 647 (red) and melanosomes pseudocolored in green from bright field images. Arrows show melanosomes internalized by keratinocytes. Scale bars = 10 μ m. (E) Quantification of melanosomes number per cell. *p* values (one-way ANOVA) were considered statistically significant when <0.05 (*), <0.01 (**) or non-significant (ns) when \geq 0.05. Plots show mean \pm SD of three independent experiments



melanosomes. We detected abundant lamellipodia and filopodia 15–20 min after the exposure to melanocores or melanosomes (Figure S4A). Thus, we decided to probe for Rho GTPase activation status 15 min after melanocore or melanosome stimulation. For this,

we used a pull-down assay that exploits the specific interaction of active Rho GTPases with PAK or Rhoketin effector proteins. Therefore, the higher the binding to PAK or Rhoketin beads, the higher the activation of Rac1/Cdc42 or RhoA, respectively. Serum starvation

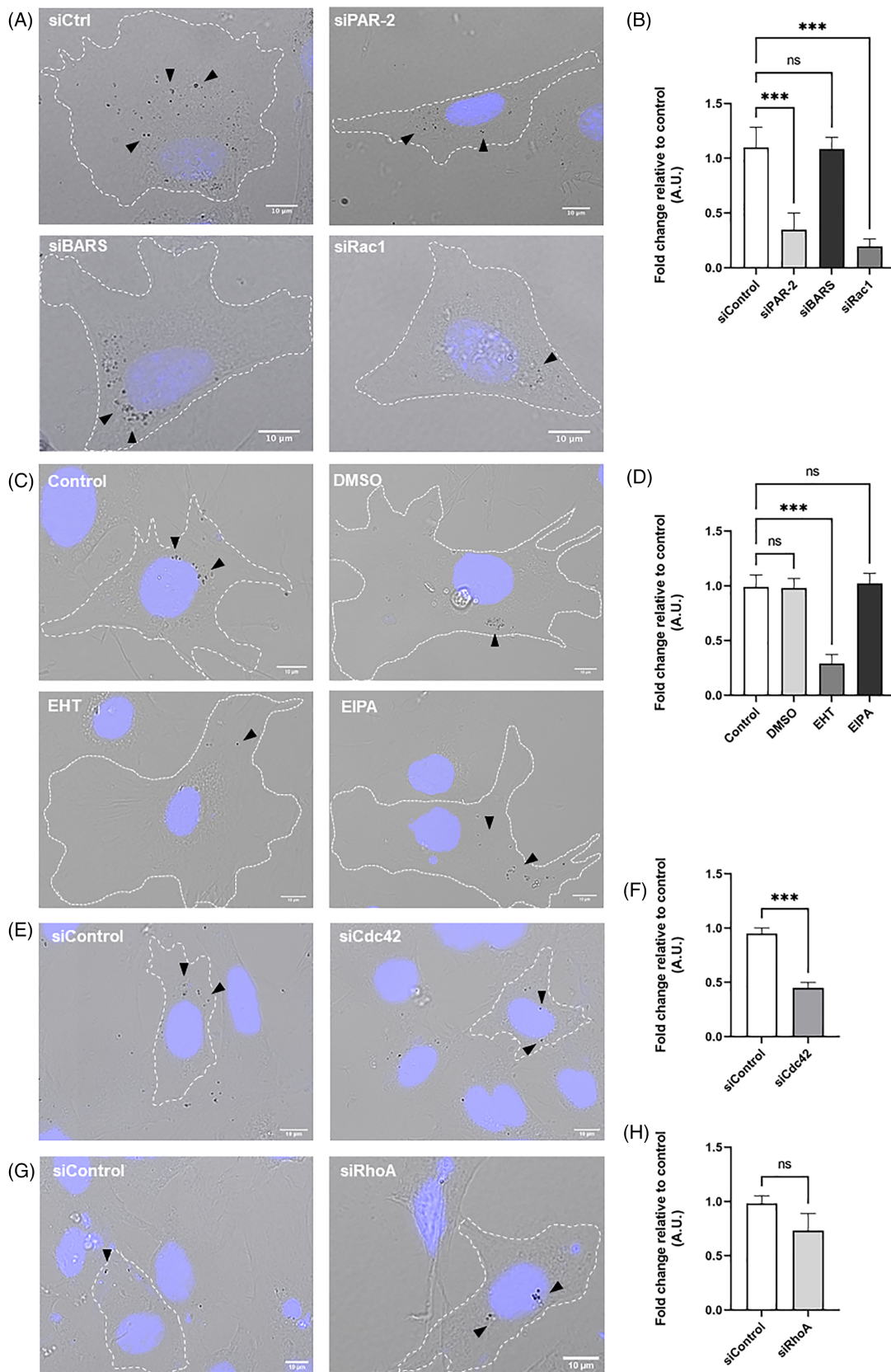


FIGURE 3 Legend on next page.

was performed to ensure reduced Rho GTPase activity prior to stimulation. Indeed, low levels of Rho GTPase activation were detected in the non-treated control (Figure 5). We loaded non-stimulated protein extracts with GTP γ S or excess GDP as positive and negative controls, respectively (Figure S4B). Upon stimulation, a modest increase in Rac1 activity was detected for both melanocores (2-fold) and melanosomes (2.7-fold) (Figure 5A). Interestingly, an increase in Cdc42 activity was observed with both melanocores and melanosomes (Figure 5B). However, the activation of Cdc42 is more striking for melanocores than for melanosomes (~7-fold vs. ~5-fold, respectively) (Figure 5B). Conversely, the increase in RhoA activity is more pronounced in melanosome-incubated cells (4.4-fold) than with melanocores (2.6-fold) (Figure 5C). Taken together, these results suggest that Rho GTPases are differently activated in the course of melanocore or melanosome internalization and support the existence of two different routes for melanin internalization, depending on the form of melanin presented to the cells.

2.4 | Melanocores and melanosomes induce PAR-2 internalization to a different extent

PAR-2 is a transmembrane receptor with an extracellular amino-terminus motif that acts as an activating ligand upon receptor cleavage. Interestingly, PAR-2 is expressed in keratinocytes but not in melanocytes and it is thought that the increase in melanin transfer and internalization that occurs upon PAR-2 activation is due to an increase in actin dynamics.^{13,16,17} To elucidate the role of PAR-2 in melanin uptake, we assessed the receptor internalization upon incubation with melanocores, melanosomes or activating/control peptides (SLIGRL/SFLLRN, respectively). For this, XB2 keratinocytes were transfected with a plasmid encoding PAR-2, FLAG-tagged at the N-terminus and HA-tagged at the C-terminus. After stimulation and internalization of the receptor, the N-terminus is cleaved, and the FLAG-tag is lost. Because our previous studies suggest that melanocores but not melanosomes are internalized in a PAR-2 dependent manner,¹⁸ we postulated that the former but not the latter can induce PAR-2 internalization. Therefore, we took advantage of this construct to determine the capacity of different types of melanin to induce receptor internalization from the plasma membrane. Indeed, after 24 h of incubation with SLIGRL peptide, which is known to activate PAR-2, the levels of FLAG at the plasma membrane decrease significantly, by approximately 20%, when compared to non-stimulated cells or cells incubated with the control peptide SFLLRN

(Figure 6D,E). These results were quantified by flow cytometry by measuring the geometric mean fluorescence intensity of FLAG at the cell surface (Figure 6A–E). Interestingly, we observed that melanocores, but not melanosomes can activate PAR-2 and induce its internalization by approximately 25% after 24 h of incubation (Figure 6C). In shorter time points (2 and 4 h), PAR-2 is internalized from the plasma membrane to a higher extent (50%) after exposure to melanocores than melanosomes (20%–30%) (Figure 6A,B). Importantly, the increase in PAR-2 internalization observed in the case of incubation with melanocores is always higher than what is observed with melanosomes. Therefore, these observations suggest that melanocores induce PAR-2 internalization and possibly its activation more robustly than melanosomes.

3 | DISCUSSION

We reported that melanocores but not melanosomes require PAR-2 to be internalized, suggesting that PAR-2 activation has specificity for non-membrane-bound melanin.¹⁸ Here, we further demonstrate that melanocores and melanosomes are internalized by keratinocytes through distinct routes and that melanocores are internalized through a PAR-2-dependent phagocytic process.

Although we observed that both melanocores and melanosomes are dependent on actin to be internalized, we present several lines of evidence suggesting that melanocore internalization is mediated by phagocytosis and melanosome uptake occurs by macropinocytosis. To distinguish between these two processes, we depleted Rac1, Cdc42, RhoA or CtBP1/BARS, which are important regulators of the aforementioned internalization routes,^{27,37} and quantified melanocore and melanosome internalization. We found that melanocore internalization is dependent on Rac1 and Cdc42, but independent of RhoA. In contrast, melanosomes are internalized in a CtBP1/BARS- and RhoA-dependent, and Rac1- and Cdc42-independent manner. Rac1 activation and membrane recruitment were described to have an important role in actin polymerization and membrane remodeling during the formation of the phagocytic cup,⁴⁴ therefore regulating the early steps of particle internalization. Moreover, Rac1 activation was also shown to be required for macropinocytic cup formation.^{31–33} Nevertheless, other proteins could compensate for Rac1 absence/inactivation, including Cdc42.⁴⁵ In addition, it was shown that Rac1-independent mechanisms can also regulate the formation of membrane ruffles,³⁴ which could explain why melanosome internalization is insensitive to Rac1 inhibition/depletion. Cdc42 is known to regulate actin polymerization and

FIGURE 3 Melanocore uptake is PAR-2-, Rac1- and Cdc42-dependent. XB2 keratinocytes were transfected with non-targeting siRNA (siCtrl), siRNA targeting PAR-2 (siPAR-2), Rac1 (siRac1) or BARS (siBARS) (A,B), Cdc42 (siCdc42) (E,F) or RhoA (siRhoA) (G,H), or treated or not with dimethyl sulfoxide (DMSO), 5-(5-(7-(Trifluoromethyl)quinolin-4-ylthio)pentyl)oxy-2-(morpholinomethyl)-4H-pyran-4-one dihydrochloride (EHT 1864; EHT) or 5-(N-ethyl-N-isopropyl)-amiloride (EIPA) (C,D). Cells were then incubated with 0.1 g/l of melanocores. The transfected cells and the cells treated with the drugs were fixed 24 h or 2 h later, respectively, and examined by bright field microscopy. Nuclei were visualized by 4',6'-diamidino-2-phenylindole (DAPI) staining (blue). Scale bars = 10 μ m. (B,F,H) Quantification of internalized melanocores/cell after a 24-h pulse. (D) Quantification of internalized melanocores/cell after a 2-h pulse. Arrowheads indicate melanocores internalized by keratinocytes. *p* values (one-way ANOVA) were considered statistically significant when <0.001 (***) or non-significant (ns) when \geq 0.05. Plots show mean \pm SD of three independent experiments.

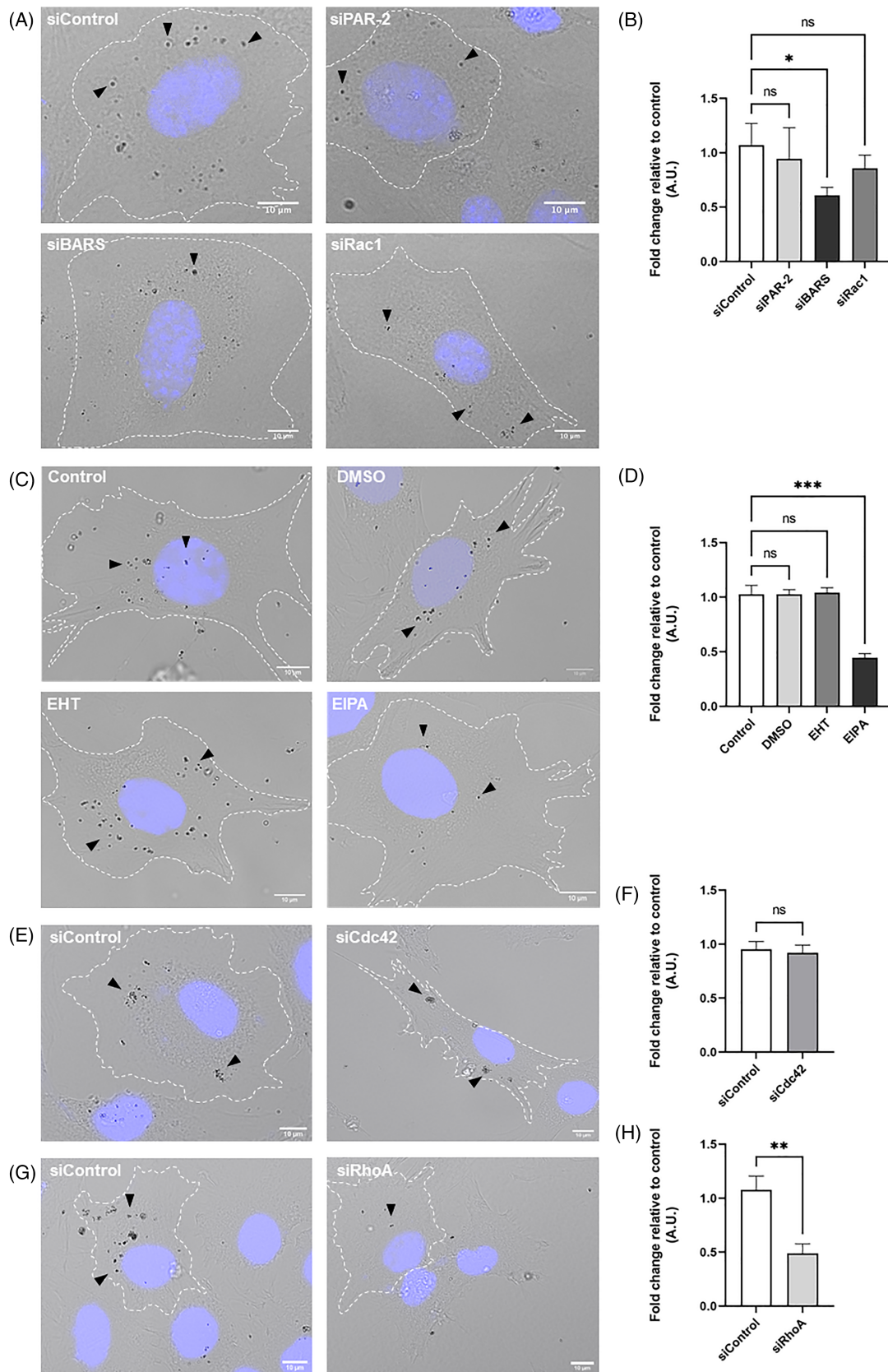
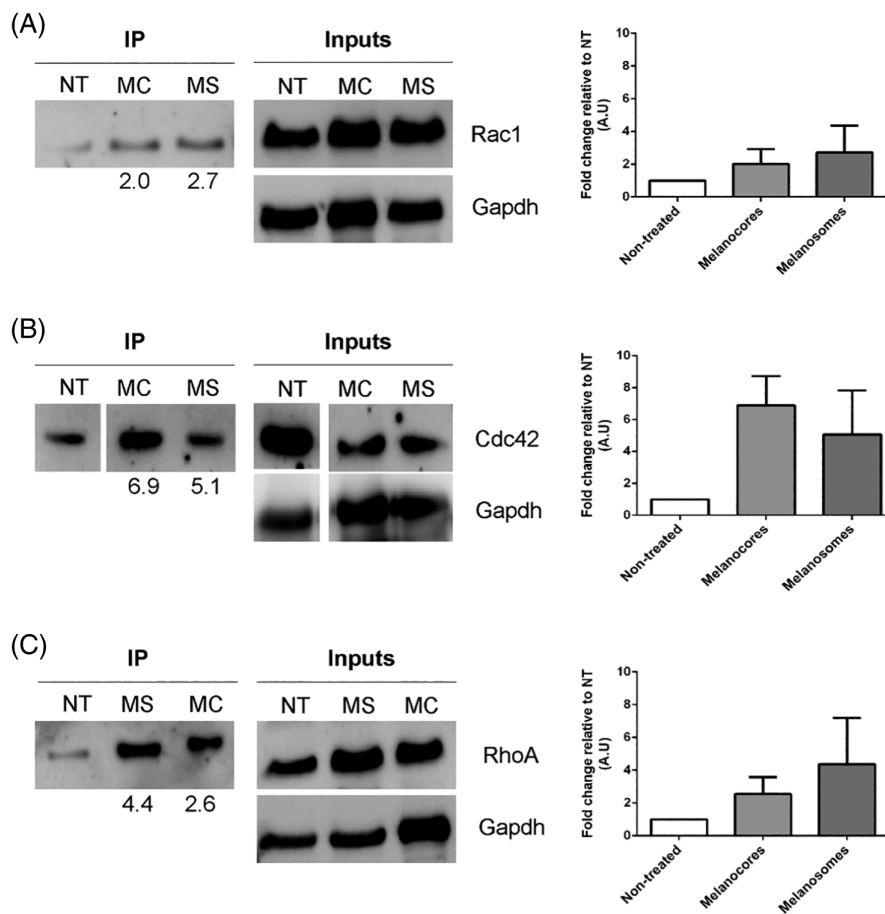


FIGURE 4 Legend on next page.

FIGURE 5 Cdc42 and RhoA are differently activated by melanocores and melanosomes. XB2 keratinocytes were incubated with melanocores or melanosomes for 15 min and lysed. Active Rho GTPases were pulled-down as described in Section 4. Quantification of the amount of active Rho GTPases (IP) was performed by normalizing to the total amount of protein (inputs) and the total amount of glyceraldehyde 3-phosphate dehydrogenase (GAPDH), as described in Section 4. (A) Active Rac1, (B) active Cdc42 and (C) active RhoA. Representative immunoblots are shown (numbers indicate fold-increase relative to non-treated). Plots show mean \pm SD of three independent experiments and represent the fold increase relative to the non-treated (NT)



pseudopod elongation during phagocytosis^{26,46} and, although its activation was shown to occur in some cell types during macropinocytosis, its requirement for this process has not been clearly established.^{32,35} This can explain why the uptake of melanocores but not melanosomes is affected by Cdc42 depletion. In the case of RhoA, it has been shown that its role in phagocytosis is receptor-dependent. In Fc receptor-mediated phagocytosis, RhoA does not seem to be required for phagocytic cup formation, whereas its activity is essential for complement receptor-mediated phagocytosis at the early stages of the process.²⁸ Furthermore, it remains controversial whether or not RhoA contributes to the late stages of phagocytosis, namely to phagosome maturation,^{28,30} which might explain the slight decrease observed in melanocore internalization upon RhoA depletion. Nonetheless, during macropinocytosis, the activity of RhoA is temporally required because it is absent from the actin-rich ring structures, and its activity peaks at the

moment of vesicle closure.³⁶ Thus, the absence of RhoA may preclude efficient internalization of melanosomes. Taken together, our results show that melanocore internalization is dependent on the presence and activation of Rac1 and Cdc42, while unaffected by EIPA treatment, strongly suggesting phagocytosis as the route taken to enter keratinocytes. Conversely, neither the absence of Rac1 or Cdc42 seems crucial for melanosome uptake. Instead, CtBP1/BARS and RhoA depletion or EIPA treatment were found to impair melanosome internalization, reinforcing the involvement of macropinocytosis in melanosome uptake.

We also investigated the activation status of Rac1, Cdc42 and RhoA after keratinocyte incubation with melanocores or melanosomes. Interestingly, we found that incubation with melanocores results in a striking increase in Cdc42 activity. These results are consistent with the impairment in melanocore internalization upon Cdc42

FIGURE 4 Melanosome uptake is CtBP1/BARS-dependent. XB2 keratinocytes were transfected with non-targeting siRNA (siCtrl), siRNA targeting PAR-2 (siPAR-2), Rac1 (siRac1) or BARS (siBARS) (A,B), Cdc42 (siCdc42) (E,F) or RhoA (siRhoA) (G,H), or treated or not with dimethyl sulfoxide (DMSO), 5-(5-(7-(Trifluoromethyl)quinolin-4-ylthio)pentyl)oxy)-2-(morpholinomethyl)-4H-pyran-4-one dihydrochloride (EHT 1864; EHT) or 5-(N-ethyl-N-isopropyl)-amiloride (EIPA) (C,D). Cells were then incubated with 0.1 g/l of melanosomes. The transfected cells and the cells treated with the drugs were fixed 24 h or 2 h later, respectively and examined by bright field microscopy. Nuclei were visualized by 4',6-diamidino-2-phenylindole (DAPI) staining (blue). Scale bars = 10 μ m. (B,F,H) Quantification of internalized melanosomes/cell after a 24-h pulse. (D) Quantification of internalized melanosomes/cell after a 2-h pulse. Arrowheads indicate melanosomes internalized by keratinocytes. *p* values (one-way ANOVA) were considered statistically significant when <0.05 (*), <0.01 (**), <0.001 (***) or non-significant (ns) when ≥ 0.05 . Plots show mean \pm SD of three independent experiments.

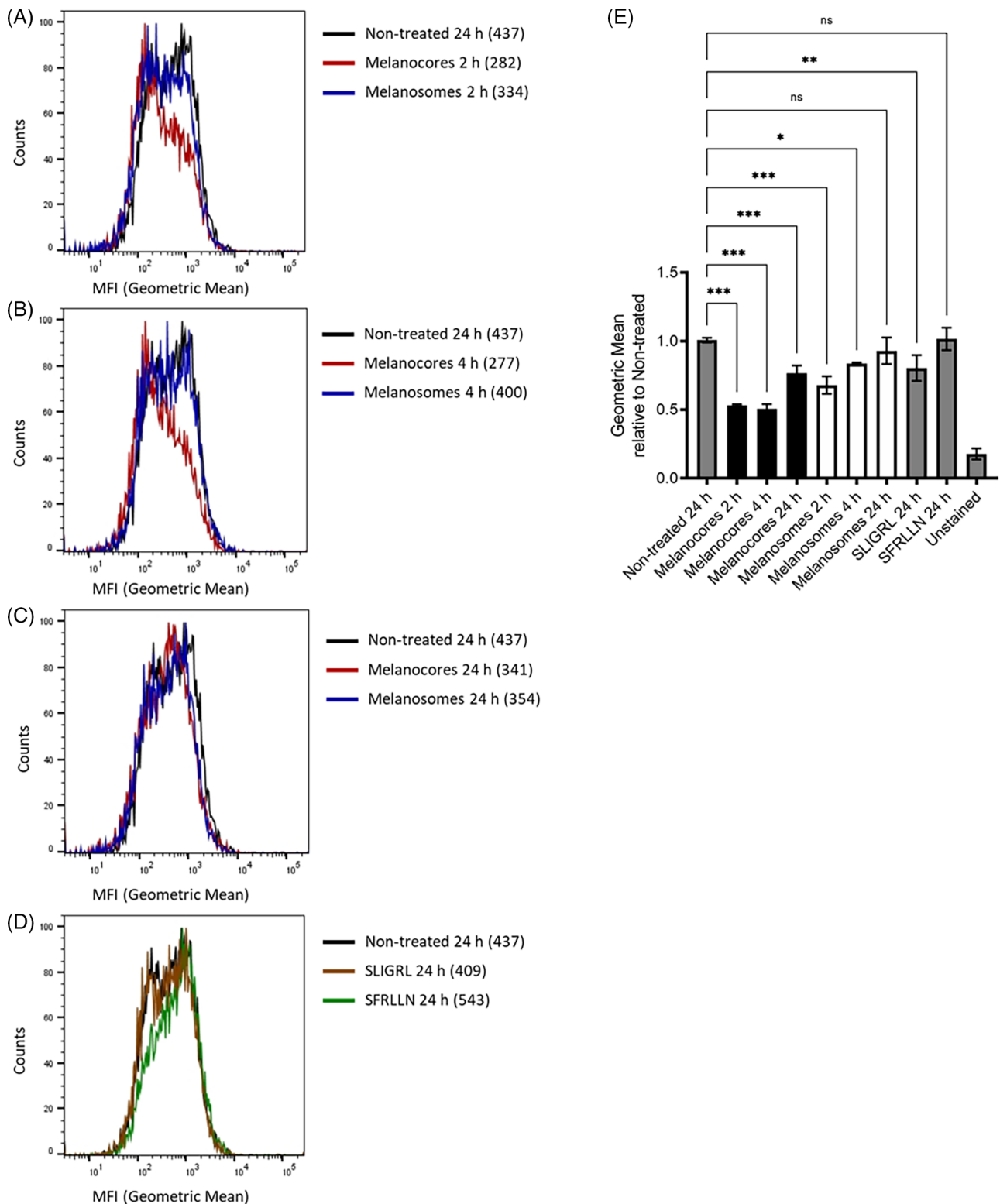


FIGURE 6 Melanocores and melanosomes induce PAR-2 internalization to a different extent. XB2 keratinocytes were transfected with FLAG-PAR-2-HA and after 24 h were incubated or not (non-treated) with melanosomes or melanocores for another 2 h (A), 4 h (B), 24 h (C), or with SFRLN or SLIGRL for 24 h (D). Then, cells were processed for flow cytometry and stained with FLAG antibody Cy3-conjugated to assess FLAG levels at the cell surface. (A–D) Representative flow cytometry plots of the mean fluorescence intensity (MFI) of the geometric mean (normalized to mode and shown in brackets) of XB2 keratinocytes after stimulation. (E) Quantification of FLAG levels at the cell surface after 2-, 4- or 24-h incubation with melanocores or melanosomes. *p* values (one-way ANOVA) were considered statistically significant when <0.05 (*), <0.01 (**), <0.01 (***) or non-significant (ns) when ≥ 0.05 . Plots show mean \pm SD of three independent experiments normalized to the values of the non-treated condition

silencing. Surprisingly, only modest Rac1 activation was found upon exposure of keratinocytes to melanosomes or melanosomes, albeit slightly higher in the case of melanosomes. Rac1 activity needs to be tightly controlled for macropinocytosis progression. In fact, Rac1 activation is important in the early steps of macropinocytosis, but the requirement for its further inactivation to allow macropinosome formation can in part explain the low activity obtained.^{32,33} Furthermore, as discussed above, Rac1-independent mechanisms can also regulate macropinocytosis.³⁴ Thus, it would be interesting to further investigate Rac1 involvement in melanosome macropinocytosis. Importantly, pseudopod formation during membrane extension in phagocytosis requires active Cdc42, followed by Rac1 activation.²⁶ Since Rac1 activation was evaluated 15 min after melanosome exposure, maximum Rac1 activity downstream of Cdc42 activation could occur after that time. Therefore, more studies of Cdc42/Rac1 activation should be performed to better characterize the sequence of events involved in melanosome phagocytosis. Finally, the modest activation of RhoA together with the results showing that its silencing does not preclude melanosome uptake, strongly suggest that melanosome phagocytosis does not require RhoA activity. Thus, our results are in agreement with a recently published study where the uptake of melanosome-rich globules under Toll-like receptor-3 (TLR-3)-stimulated conditions was shown to be dependent of RhoA activation but independent of PAR-2.⁴⁷ PAR-2-stimulation catalyzes the conversion of ATP to cAMP, which activates Rac1 and subsequently inactivates RhoA.^{17,48} This PAR-2-mediated activation/inactivation of Rac1/RhoA may thus be a critical factor in melanosome uptake. Nevertheless, the fact that TLR-3 activation leads to an increase in PAR-2 expression might explain the increase in phagocytic activity of keratinocytes, as previously reported.^{17,40}

We also assessed the ability of melanosomes and melanosomes to induce PAR-2 internalization. Melanosomes induce endocytosis of the receptor in a more robust and sustained manner than melanosomes, suggesting a mechanism in which melanosomes are internalized by phagocytosis in a Rac1/Cdc42-dependent manner upon internalization of PAR-2, as opposed to melanosomes, which are internalized through macropinocytosis independently of PAR-2. Thus, PAR-2 could be essential to prepare for the formation of the phagocytic cup that engulfs melanosomes during their internalization by keratinocytes.

How melanin is presented to keratinocytes, that is, the presence or absence of membrane surrounding the melanin core is therefore critically important to define the route of internalization. We speculate that melanosome transfer through coupled exocytosis/phagocytosis occurs preferentially at basal levels of pigmentation and is the main mode of transfer, while the transfer of melanosome-laden globules could be used in stress conditions, for instance during tanning to ensure a high throughput of pigment transfer.¹¹ Even though a potential caveat of our study is the use of mouse keratinocytes and melanin isolated from human MNT-1 melanoma cells, it is important to mention that this *in vitro* melanin uptake assay was validated by others using human primary keratinocytes,⁴⁹ further supporting the relevance of our model and our observations. In conclusion, our current results and previously published studies suggest that the main mechanism of pigment transfer

in the skin epidermis involves coupled exo/phagocytosis of melanosomes, regulated by PAR-2.

4 | MATERIALS AND METHODS

4.1 | Cell culture and reagents

Mouse keratinocytes (XB2 cell line), obtained from Dorothy Bennett and Elena Sviderskaya lab, were cultured in DMEM supplemented with 10% FBS, 2 mM L-glutamine, 100 U/ml penicillin and 100 µg/ml streptomycin. Cells were maintained in a humidified incubator at 37°C and 10% CO₂. MNT-1 human melanoma cells were maintained in DMEM containing 10% FBS, 2 mM L-glutamine, non-essential amino acids, sodium pyruvate, 100 U/ml penicillin and 100 µg/ml streptomycin. SLIGRL-NH₂, SFLLRN and synthetic melanin were purchased from Sigma (Darmstadt, Germany), and melanin from *Sepia officinalis* from Santa Cruz (Dallas, TX, USA).

4.2 | Melanosome preparation and uptake assay

Melanosomes were prepared as described previously.¹⁸ MNT-1 cells were cultured in 150 cm² flasks (Corning, NY, USA) for 5 days. Conditioned medium was collected and centrifuged at 300g for 5 min to pellet floating cells. The supernatant was then transferred to a clean tube and centrifuged for 1 h, and concentrated in a vivaspin Centricon (Sigma) with a pore size of 300 000 Da at 2683g. Melanosome solution absorbance was measured using a Nanodrop 2000 (Thermo Fisher Scientific, Waltham, MA, USA) at 340 nm and the concentration calculated according to a calibration curve developed in-house (Absorbance = 1.8546 × Concentration [g/l] – 0.0422). For internalization studies, a concentration of 0.1 g/l of melanosomes was used, unless otherwise stated.

XB2 keratinocytes were fed with 0.1 g/l of melanosomes or melanosomes and incubated at 37°C and 10% CO₂ for different times. Cells were then washed three times with PBS and fixed with 4% paraformaldehyde (PFA; Electron Microscopy Sciences, PA, USA) in PBS for 20 min at room temperature. The number of melanosomes per cell was counted and the mean calculated. Nuclei were counted to ensure similar cell confluence in all samples and the amount of melanin internalized per cell calculated. In the assays using inhibitors, cells were incubated with EIPA (Tocris, MN, USA; 50 µM) or EHT 1864 (Santa Cruz Biotechnology, Dallas, TX, USA; 20 µM), before being fed with melanosomes (0.1 g/l), melanosomes or Rhodamine B isothiocyanate–dextran 70 kDa (Sigma, Darmstadt, Germany; 0.1 µg/µl) for 2 h and processed for immunofluorescence, as described below. In the experiments with dextran, we imaged the samples less than 16 h after fixation. To confirm that we are not underestimating internalized dextran levels because of fixation, we also performed experiments using live cell imaging. The dextran signal in fixed control cells was similar to that of cells imaged live, and similar results were obtained upon BARS silencing or EIPA treatment

(not shown). The timepoints for the EHT 1864 and EIPA treatments were optimized by incubating the cells with the drugs for long (16 h), medium (4 h) and short (20 min) timepoints, before being fed with either melanocores or melanosomes. Melanin uptake was then analyzed, as well as structural/morphological differences and cell death, and the best timepoint for each drug was chosen. In parallel, melanin-fed cells were stained with anti-PMEL antibody (HMB45) (Agilent DAKO, CA, USA), to allow the detection of internalized melanin by confocal microscopy and quantification using the Spot Detector plugin from Icy Software (<https://icy.bioimageanalysis.org>).

4.3 | Melanosome preparation

Melanosomes were prepared as described previously.⁵⁰ Briefly, MNT-1 cells were scraped in H buffer (50 mM imidazole, pH 7.4, 250 mM sucrose, 1 mM ethylenediamine tetraacetic acid [EDTA], 0.5 mM ethylene glycol tetraacetic acid [EGTA], 5 mM MgSO₄, 0.15 mg/ml casein and 1 mM dithiothreitol) and homogenized by passing several times through a cell cracker 26G needle. The post-nuclear supernatant (PNS) was obtained by centrifugation at 600g for 5 min. The PNS was then centrifuged at 2500g for 5 min. The recovered pellet was added onto a 50% Percoll cushion, centrifuged at 5000g for 20 min, and the pellet of melanosomes collected.

4.4 | Transmission electron microscopy

For transmission electron microscopy analysis of purified melanin, 200 μ l of either melanocore or melanosome preparations were pelleted by centrifugation at 2400g for 15 min, before resuspending pellets in 2% PFA and 2% glutaraldehyde (both from TAAB) in 0.1 M phosphate buffer (PB). Melanin was fixed in suspension for 2 h at room temperature, washed three times with PB, and osmicated for 1 h on ice using 1% osmium tetroxide and 1.5% potassium ferrocyanide in distilled water. Pellets were subsequently washed with distilled water and dehydrated with a series of increasing ethanol concentrations (70%, 90%, 2 \times 100%) before infiltrating and embedding in epoxy resin. After polymerizing at 70°C overnight, resin blocks were sectioned at 80 nm using a UC7 ultramicrotome (Leica) and a diamond knife (Diatome), and sections collected on formvar/carbon-coated copper mesh grids (Agar Scientific, Stansted, UK). Sections on grids were post-stained with lead citrate and imaged using a Hitachi H-7650 TEM with an AMT XR41M digital camera.

4.5 | Rho GTPase activation assay

The experiment was performed using the RhoA/Rac1/Cdc42 Activation Assay Combo Biochem Kit™ (Cytoskeleton, Cat. # BK030)

according to the manufacturer's instructions. Briefly, XB2 cells were plated in six-well plates at a density of 1×10^5 cells/well. Then, the complete media was changed to DMEM supplemented with 1% FBS for 2 days to synchronize the cells. Twenty-four hours before stimulation, DMEM without serum was added to inactivate Rho GTPases. Melanocores or melanosomes were then added, and the plate was centrifuged at 60g for 1 min, followed by incubation at 37°C for 15 min. After incubation, cells were quickly lysed on ice and protein extracts snap-frozen using liquid nitrogen. Immunoprecipitation was performed using the PAK- and Rhoketin-beads included in the kit. Non-treated XB2 cells were loaded with 200 μ M GTP γ S or excess GDP (1 mM) as pull-down controls. Lysates were then loaded on 12% SDS-acrylamide gels, transferred to nitrocellulose membrane (GE Healthcare Life Sciences) for 50 min at 100 V and processed for Western blotting. Membranes were blocked with 5% milk in Tris-buffered saline (TBS) with 0.05% Tween-20 and incubated with primary antibodies included in the kit, followed by horseradish peroxidase (HRP)-conjugated secondary anti-mouse or anti-goat antibodies. HRP activity was probed with Amersham ECL Select or Prime (GE Healthcare Life Sciences), according to the manufacturer's instructions. Chemiluminescence was detected using a ChemiDoc™ Touch Imaging and the results analyzed with ImageLab software. Incubation with anti-glyceraldehyde 3-phosphate dehydrogenase (anti-GAPDH) antibody in 5% milk in TBS with 0.05% Tween was done to normalize the amount of protein present in each condition (input). Densitometric quantification was performed using ImageJ. Furthermore, quantification of the amount of active Rho GTPases (IP) was performed by normalizing to the total amount of each GTPase (inputs) and the total amount of protein (GAPDH) (IP/[input/GAPDH]). Results are presented as the mean fold-increase relative to the non-treated control.

4.6 | Immunofluorescence microscopy

Cells were grown on coverslips for immunofluorescence and fixed in 4% PFA in PBS for 20 min at room temperature. Cells were blocked and permeabilized with 1% bovine serum albumin (Sigma) and 0.05% saponin (Sigma) in PBS for 30 min. Fixed cells were then incubated with primary antibodies for 1 h and then for a further 1 h with appropriate secondary antibodies conjugated with a fluorophore (Molecular Probes). The antibodies used and respective dilutions are displayed in Table S1. Coverslips were finally mounted in MOWIOL mounting medium (Calbiochem). All antibody incubations and washes were done with 1 \times PBS, 0.5% BSA and 0.05% saponin. To visualize the nuclei, cells were incubated with 4',6-diamidino-2-phenylindole (DAPI) (Invitrogen) for 5 min. Images were acquired on a Zeiss Observer Z2 widefield microscope, equipped with a Zeiss 506 Mono camera using the 63 \times 1.4 NA Oil objective or a Zeiss LSM 710 confocal microscope with a Plan-Apochromat 63 \times 1.4 NA oil-immersion objective. Images were processed using

ImageJ and Adobe Illustrator 6.0 (Adobe, San Jose, CA, USA) software.

4.7 | Flow cytometry

To prepare XB2 keratinocytes for flow cytometry, cells were washed with PBS and fluorescence-activated cell sorter (FACS) buffer (1% FBS [v/v] and 2 mM EDTA in PBS), centrifuged at 300g for 5 min and resuspended in 200 μ l FACS buffer. Cells were incubated with anti-FLAG-Cy3 (Sigma) antibody, diluted 1:50 in FACS buffer for 1 h, at 4°C to ensure that internalization was blocked. Cells were then washed with FACS buffer, centrifuged at 300g for 5 min and resuspended with 200 μ l FACS buffer. Data acquisition was performed in a FACS CANTO II flow cytometer (BDBiosciences) At least 30 000 cells were acquired per condition using BD FACSDiva™ software (Version 6.1.3, BD Biosciences). Data analysis was performed in FlowJo (Version 10, BD Biosciences).

4.8 | Actin polymerization inhibition assay

XB2 keratinocytes (5×10^4) were treated with 0.02 μ g/ml Lantrunculin A (Sigma) or 0.05 μ g/ml Cytochalasin D (Sigma), both diluted in DMSO or non-treated for 1 h and then incubated at the same time with melanosomes or melanosomes for 24 h. Cells were then washed and left to recover for 1 h in complete growth medium before fixation with 4% PFA in PBS. Nuclei were visualized by DAPI staining, and filamentous (F)-actin was stained with Phalloidin 568.

4.9 | Plasmid transfection

XB2 mouse keratinocytes (4×10^4) cultured in 24-well plates (Corning, NY, USA) and transfected with 1 μ g of pEGFP-FLAG-PAR-2-HA mixed with 1.5 μ l of TurboFect (Thermo Fisher Scientific) in 200 μ l of Opti-MEM (Gibco) according to the manufacturer's instructions. Cells were incubated for 24 h at 37°C and then the medium was changed to 500 μ l complete XB2 medium.

4.10 | siRNA silencing

XB2 keratinocytes (1×10^5 per well) were seeded in 24-well plates (Corning, NY, USA). Twenty-four hours later, 50 nM of gene-specific siGenome SMART pool (Thermo Fisher Scientific) was diluted in 32 μ l Opti-MEM (Gibco), while 1.2 μ l of Dharmafect 1 (Dharmacon, GELifeScience) was added to 6 μ l of Opti-MEM. These mixtures were combined and incubated at room temperature for 20 min. Finally, 160 μ l of Opti-MEM was added to the mixture, the medium was removed from the cells, and the siRNA mixture added to each well. Cells were incubated for 24 h at 37°C and then the medium was changed to complete medium. Non-targeting siRNA pool (Thermo Scientific) was used as control.

4.11 | Real-time quantitative polymerase chain reaction

Total RNA was isolated from cells using RNeasy Mini kit (Qiagen) and reverse-transcribed to cDNA using SuperScript® II (Invitrogen), according to the manufacturer's instructions. Real-time quantitative polymerase chain reaction reactions were performed using a Roche LightCycler equipment (Roche) and Roche SybrGreen Master Mix reagent (SybrGreen, Roche). Five microliters of SybrGreen and 4 μ l of cDNA together with 10 μ M of appropriate primers were used per well, in triplicate, for a total reaction volume of 10 μ l. For each protein, gene expression was calculated relative to control wells and normalized for GAPDH (used as housekeeping gene), using LightCycler96 software (Roche) to analyze the results. The primers used are shown in Table S2.

4.12 | Statistical analysis

Statistical analysis was performed using Prism software (GraphPad Software Inc.). One-way ANOVA was used to analyze the *p* value of the differences obtained.

ACKNOWLEDGMENTS

The authors would like to thank the scientific and technical assistance from the CEDOC Cell Culture, Flow Cytometry and Microscopy facilities. We also thank the Electron Microscopy Facility of Instituto Gulbenkian de Ciência for technical assistance. The authors also thank Dorothy Bennett and Elena Sviderskaya (St. George's University of London, UK), Susana Lopes (CEDOC, NOVA Medical School) and Paulo Matos (National Health Institute Doutor Ricardo Jorge, Portugal) for the kind gift of reagents and Paulo Matos also for expert advice. This article was supported by the LYSOCIL project. This project has received funding from the European Union's Horizon 2020 research and innovation program under grant agreement No. 811087. This article was also supported by Fundação para a Ciência e a Tecnologia (FCT), Portugal through grant PTDC/BIA-CEL/29765/2017, PhD fellowships to HM, MVN, LBL and LCC (PD/BD/114118/2015, PD/BD/137442/2018, SFRH/BD/131938/2017 and 2020.8812.BD, respectively), the FCT Investigator Program to DCB (IF/00501/2014/CP1252/CT0001), and FCT Unit iNOVA4Health – UIDB/04462/2020 and UIDP/04462/2020, a programme financially supported by FCT / Ministério da Ciência, Tecnologia e Ensino Superior, through national funds.

CONFLICT OF INTEREST

The authors declare no conflict of interest.









PEER REVIEW

The peer review history for this article is available at <https://publons.com/publon/10.1111/tra.12843>.

DATA AVAILABILITY STATEMENT

The authors confirm that the data supporting the findings of this study are available within the article and its supplementary materials.

ORCID

Hugo Moreiras  <https://orcid.org/0000-0003-0984-7921>
 Liliana Bento-Lopes  <https://orcid.org/0000-0002-6893-610X>
 Cristina Escrevente  <https://orcid.org/0000-0002-2183-3947>
 Luís C. Cabaço  <https://orcid.org/0000-0003-0976-1781>
 Michael J. Hall  <https://orcid.org/0000-0002-1579-1488>
 José S. Ramalho  <https://orcid.org/0000-0002-1927-164X>
 Miguel C. Seabra  <https://orcid.org/0000-0002-6404-4892>
 Duarte C. Barral  <https://orcid.org/0000-0001-8867-2407>

REFERENCES

- Lin JY, Fisher DE. Melanocyte biology and skin pigmentation. *Nature*. 2007;445(7130):843-850. doi:10.1038/nature05660
- Lai-Cheong JE, McGrath JA. Structure and function of skin, hair and nails. *Medicine*. 2013;41(6):317-320. doi:10.1016/j.mpmed.2013.04.017
- Nicol NH. Anatomy and physiology of the skin. *Dermatol Nurs*. 2005;17(1):62. doi:10.4324/9780203450505_chapter_1
- Marks MS, Seabra MC. The melanosome: membrane dynamics in black and white. *Nat Rev Mol Cell Biol*. 2001;2(10):738-748. doi:10.1038/35096009
- Wasmeier C, Hume AN, Bolasco G, Seabra MC. Melanosomes at a glance. *J Cell Sci*. 2008;121(24):3995-3999. doi:10.1242/jcs.040667
- Raposo G, Marks MS. Melanosomes – dark organelles enlighten endosomal membrane transport. *Nature Reviews Molecular Cell Biology*. 2007;8(10):786-797. doi:10.1038/nrm2258
- Delevoye C, Marks MS, Raposo G. Lysosome-related organelles as functional adaptations of the endolysosomal system. *Curr Opin Cell Biol*. 2019;59:147-158. doi:10.1016/j.cob.2019.05.003
- Wu X, Hammer JA. Melanosome transfer: it is best to give and receive. *Curr Opin Cell Biol*. 2014;29(1):1-7. doi:10.1016/j.cob.2014.02.003
- Van Den Bossche K, Naeyaert JM, Lambert J. The quest for the mechanism of melanin transfer. *Traffic*. 2006;7(7):769-778. doi:10.1111/j.1600-0854.2006.00425.x
- Yoshida Y, Hachiya A, Sriwiriyanont P, et al. Functional analysis of keratinocytes in skin color using a human skin substitute model composed of cells derived from different skin pigmentation types. *FASEB J*. 2007;21(11):2829-2839. doi:10.1096/fj.06-6845com
- Moreiras H, Seabra MC, Barral DC. Melanin Transfer in the Epidermis: The Pursuit of Skin Pigmentation Control Mechanisms. *Int J Mol Sci*. 2021;22(9):4466. doi:10.3390/ijms22094466
- Benito-Martinez S, Salavessa L, Raposo G, Marks MS, Delevoye C. Melanin transfer and fate within keratinocytes in human skin pigmentation. *Integr Comp Biol*. 2021;21:1-23. doi:10.1093/icb/icab094
- Seiberg M, Paine C, Sharlow E, et al. The protease-activated receptor 2 regulates pigmentation via keratinocyte-melanocyte interactions. *Exp Cell Res*. 2000;254(1):25-32. doi:10.1006/excr.1999.4692
- Seiberg M, Paine C, Sharlow E, et al. Inhibition of melanosome transfer results in skin lightening. *J Invest Dermatol*. 2000;115(2):162-167. doi:10.1046/j.1523-1747.2000.00035.x
- Lin CB, Chen N, Scarpa R, et al. LIGR, a protease-activated receptor-2-derived peptide, enhances skin pigmentation without inducing inflammatory processes. *Pigment Cell Melanoma Res*. 2008;21(2):172-183. doi:10.1111/j.1755-148X.2008.00441.x
- Sharlow ER, Paine CS, Babiarz L, Eisinger M, Shapiro S, Seiberg M. The protease-activated receptor-2 upregulates keratinocyte phagocytosis. *J Cell Sci*. 2000;113(17):3093-3101.
- Scott G, Leopardi S, Parker L, Babiarz L, Seiberg M, Han R. The proteinase-activated receptor-2 mediates phagocytosis in a Rho-dependent manner in human keratinocytes. *J Invest Dermatol*. 2003;121(3):529-541. doi:10.1046/j.1523-1747.2003.12427.x
- Correia MS, Moreiras H, Pereira FJCC, et al. Melanin transferred to keratinocytes resides in nondegradative endocytic compartments. *J Invest Dermatol*. 2018;138(3):637-646. doi:10.1016/j.jid.2017.09.042
- Tadokoro R, Murai H, Sakai KI, Okui T, Yokota Y, Takahashi Y. Melanosome transfer to keratinocyte in the chicken embryonic skin is mediated by vesicle release associated with Rho-regulated membrane blebbing. *Sci Rep*. 2016;6(April):1-11. doi:10.1038/srep38277
- Thong H-Y, Jee S-H, Sun C-C, Boissy RE. The patterns of melanosome distribution in keratinocytes of human skin as one determining factor of skin colour. *Br J Dermatol*. 2003;149(3):498-505. doi:10.1046/j.1365-2133.2003.05473.x
- Paul D, Achouri S, Yoon YZ, Herre J, Bryant CE, Cicuta P. Phagocytosis dynamics depends on target shape. *Biophys J*. 2013;105(5):1143-1150. doi:10.1016/j.bpj.2013.07.036
- Hirota K, Ter H. Endocytosis of particle formulations by macrophages and its application to clinical treatment. *Molecular Regulation of Endocytosis*. InTech; London: InTech Open; 2012:413-428. doi:10.5772/45820
- Jaffe AB, Hall A. Rho GTPases: biochemistry and biology. *Annu Rev Cell Dev Biol*. 2005;21:247-269. doi:10.1146/annurev.cellbio.21.020604.150721
- Olayioye MA, Noll B, Hausser A. Spatiotemporal Control of Intracellular Membrane Trafficking by Rho GTPases. *Cells*. 2019;8(12):1478. doi:10.3390/cells8121478
- Mylvaganam S, Freeman SA, Grinstein S. The cytoskeleton in phagocytosis and macropinocytosis. *Curr Biol*. 2021;31(10):R619-R632. doi:10.1016/j.cub.2021.01.036
- Hoppe AD, Swanson JA. Cdc42, Rac1, and Rac2 display distinct patterns of activation during phagocytosis. *Mol Biol Cell*. 2004;15(8):3509-3519. doi:10.1091/mbc.e03-11-0847
- Groves E, Dart AE, Covarelli V, Caron E. Molecular mechanisms of phagocytic uptake in mammalian cells. *Cell Mol Life Sci*. 2008;65(13):1957-1976. doi:10.1007/s00018-008-7578-4
- Caron E, Hall A. Identification of two distinct mechanisms of phagocytosis controlled by different Rho GTPases. *Science*. 1998;282(5394):1717-1721. doi:10.1126/science.282.5394.1717
- Erwig L-P, McPhillips KA, Wynes MW, Ivetic A, Ridley AJ, Henson PM. Differential regulation of phagosome maturation in macrophages and dendritic cells mediated by Rho GTPases and ezrin-radixin-moesin (ERM) proteins. *Proc Natl Acad Sci USA*. 2006;103(34):12825-12830. doi:10.1073/pnas.0605331103
- Olazabal IM, Caron E, May RC, Schilling K, Knecht DA, Machesky LM. Rho-kinase and myosin-II control phagocytic cup formation during CR, but not FcγR, phagocytosis. *Curr Biol*. 2002;12(16):1413-1418. doi:10.1016/s0960-9822(02)01069-2
- Veltman DM, Williams TD, Bloomfield G, Chen BC, Betzig E, Insall RH, Kay RR. A plasma membrane template for macropinocytic cups. *eLife*. 2016;5:e20085. doi:10.7554/eLife.20085
- Egami Y, Taguchi T, Maekawa M, Arai H, Araki N. Small GTPases and phosphoinositides in the regulatory mechanisms of macropinosome formation and maturation. *Front Physiol*. 2014;5:374. doi:10.3389/fphys.2014.00374
- Fujii M, Kawai K, Egami Y, Araki N. Dissecting the roles of Rac1 activation and deactivation in macropinocytosis using microscopic photomanipulation. *Sci Rep*. 2013;3:1-10. doi:10.1038/srep02385
- West MA, Prescott AR, Eskelinen EL, Ridley AJ, Watts C. Rac is required for constitutive macropinocytosis by dendritic cells but does not control its downregulation. *Curr Biol*. 2000;10(14):839-848. doi:10.1016/s0960-9822(00)00595-9
- Patel JC, Galán JE. Differential activation and function of Rho GTPases during *Salmonella*-host cell interactions. *J Cell Biol*. 2006;175(3):453-463. doi:10.1083/jcb.200605144
- Zawistowski JS, Sabouri-Ghomi M, Danuser G, Hahn KM, Hodgson L. A RhoC biosensor reveals differences in the activation kinetics of

- RhoA and RhoC in migrating cells. *PLoS One*. 2013;8(11):e79877. doi:[10.1371/journal.pone.0079877](https://doi.org/10.1371/journal.pone.0079877)
37. Kerr MC, Teasdale RD. Defining macropinocytosis. *Traffic*. 2009;10(4):364-371. doi:[10.1111/j.1600-0854.2009.00878.x](https://doi.org/10.1111/j.1600-0854.2009.00878.x)
38. Liberali P, Kakkonen E, Turacchio G, et al. The closure of Pak1-dependent macropinosomes requires the phosphorylation of CtBP1/BARS. *EMBO J*. 2008;27(7):970-981. doi:[10.1038/emboj.2008.59](https://doi.org/10.1038/emboj.2008.59)
39. Koivusalo M, Welch C, Hayashi H, et al. Amiloride inhibits macropinocytosis by lowering submembranous pH and preventing Rac1 and Cdc42 signaling. *J Cell Biol*. 2010;188(4):547-563. doi:[10.1083/jcb.200908086](https://doi.org/10.1083/jcb.200908086)
40. Wolff K, Konrad K. Phagocytosis of latex beads by epidermal keratinocytes in vivo. *J Ultrastruct Res*. 1972;39(3-4):262-280. doi:[10.1016/S0022-5320\(72\)90022-6](https://doi.org/10.1016/S0022-5320(72)90022-6)
41. Potter B, Medenica M. Ultramicroscopic phagocytosis of synthetic melanin by epidermal cells in vivo. *J Invest Dermatol*. 1968;51(4):300-303. doi:[10.1038/jid.1968.132](https://doi.org/10.1038/jid.1968.132)
42. Li L, Wan T, Wan M, Liu B, Cheng R, Zhang R. The effect of the size of fluorescent dextran on its endocytic pathway. *Cell Biol Int*. 2015;39(5):531-539. doi:[10.1002/cbin.10424](https://doi.org/10.1002/cbin.10424)
43. Nobes CD, Hall A. Rho, rac, and cdc42 GTPases regulate the assembly of multimolecular focal complexes associated with actin stress fibers, lamellipodia, and filopodia. *Cell*. 1995;81(1):53-62. doi:[10.1016/0092-8674\(95\)90370-4](https://doi.org/10.1016/0092-8674(95)90370-4)
44. Castellano F, Montcourrier P, Chavrier P. Membrane recruitment of Rac1 triggers phagocytosis. *J Cell Sci*. 2000;113(17):2955-2961.
45. Bonfim-Melo A, Ferreira ÉR, Mortara RA. Rac1/WAVE2 and Cdc42/N-WASP participation in actin-dependent host cell invasion by extracellular amastigotes of *Trypanosoma cruzi*. *Front Microbiol*. 2018;9:360. doi:[10.3389/fmicb.2018.00360](https://doi.org/10.3389/fmicb.2018.00360)
46. Lorenzi R, Brickell PM, Katz DR, Kinnon C, Thrasher AJ. Wiskott-Aldrich syndrome protein is necessary for efficient IgG-mediated phagocytosis. *Blood*. 2000;95(9):2943-2946. <http://www.ncbi.nlm.nih.gov/pubmed/10779443>
47. Koike S, Yamasaki K, Yamauchi T, et al. TLR3 stimulation induces melanosome endo/phagocytosis through RHOA and CDC42 in human epidermal keratinocyte. *J Dermatol Sci*. 2019;96(3):168-177. doi:[10.1016/j.jdermsci.2019.11.005](https://doi.org/10.1016/j.jdermsci.2019.11.005)
48. Scott G, Leopardi S. The cAMP signaling pathway has opposing effects on Rac and Rho in B16F10 cells: implications for dendrite formation in melanocytic cells. *Pigment Cell Res*. 2003;16(2):139-148. doi:[10.1034/j.1600-0749.2003.00022.x](https://doi.org/10.1034/j.1600-0749.2003.00022.x)
49. Benito-Martínez S, Zhu Y, Jani RA, Harper DC, Marks MS, Delevoye C. Research techniques made simple: cell biology methods for the analysis of pigmentation. *J Invest Dermatol*. 2020;140(2):257-268.e8. doi:[10.1016/j.jid.2019.12.002](https://doi.org/10.1016/j.jid.2019.12.002)
50. Chabrilat ML, Wilhelm C, Wasmeier C, Sviderskaya EV, Louvard D, Coudrier E. Rab8 regulates the actin-based movement of melanosomes. *Mol Biol Cell*. 2005;16(4):1640-1650. doi:[10.1091/mbc.E04-09-0770](https://doi.org/10.1091/mbc.E04-09-0770)

SUPPORTING INFORMATION

Additional supporting information may be found in the online version of the article at the publisher's website.

How to cite this article: Moreiras H, Bento-Lopes L, Neto MV, et al. Melanocore uptake by keratinocytes occurs through phagocytosis and involves protease-activated receptor-2 internalization. *Traffic*. 2022;23(6):331-345. doi:[10.1111/tra.12843](https://doi.org/10.1111/tra.12843)